ACS APPLIED MATERIALS & INTERFACES

Research Article

www.acsami.org

High Rate Performance of Flexible Pseudocapacitors fabricated using Ionic-Liquid-Based Proton Conducting Polymer Electrolyte with Poly(3, 4-ethylenedioxythiophene):Poly(styrene sulfonate) and Its Hydrous Ruthenium Oxide Composite Electrodes

Sellam and S. A. Hashmi*

Department of Physics & Astrophysics, University of Delhi, Delhi 110007, India

ABSTRACT: We report the studies on all-solid-state flexible pseudocapacitors based on poly (3,4-ethylenedioxythiophene)-poly (styrene sulfonate) (PEDOT-PSS) and PEDOT-PSS/hydrous ruthenium oxide composite electrodes separated by nonaqueous proton conducting polymer electrolyte. Structural, thermal and electrochemical properties including high ionic conductivity (6.2×10^{-2} S cm^{-1} at 20 °C) of the polymer electrolyte, comprising ionic liquid 1-ethyl 3-methyl imidazolium hydrogen sulfate ($EMIHSO_4$) immobilized in the blend of poly (vinyl alcohol) (PVA) and poly (vinyl pyrrolidone) (PVP), demonstrate its excellent suitability in supercapacitor fabrication. A substantial improvement in the specific capacitance (hence the specific energy) has been obtained when the PEDOT-PSS electrodes in the symmetrical pseudocapacitor are replaced by the composite electrodes PEDOT-PSS/$RuO_2{\cdot}xH_2O$. High rate capability of the capacitor cell (with PEDOT-PSS electrodes) has been observed, as evidenced from the high knee frequency (~966 Hz), low response time (~70 ms) and high pulse power (~10.2 kW kg^{-1}), observed by impedance analysis. Almost rectangular (capacitive) cyclic voltammetric patterns for high scan rates (up to 15 V s^{-1}) confirm the high rate performance of the pseudocapacitor. The PEDOT-PSS/$RuO_2{\cdot}xH_2O$ composite electrodes show the lower rate capability (knee frequency ~312 Hz, response time ~1 s, pulse power ~3.2 kW kg^{-1} and capacitive CV response up to 500 mV s^{-1}) because of slow exchange of charges at the interfaces via $RuO_2{\cdot}xH_2O$. However, the pseudocapacitor with composite electrodes shows higher rate performance relative to many reported $RuO_2{\cdot}xH_2O$ systems. About 15% improvement is noticed in the capacitance value when the capacitor with composite electrodes is initially charged and discharged up to ~200 cycles. Thereafter, the cell shows almost constant value of specific capacitance (~70 F g^{-1}) for 1000 cycles.

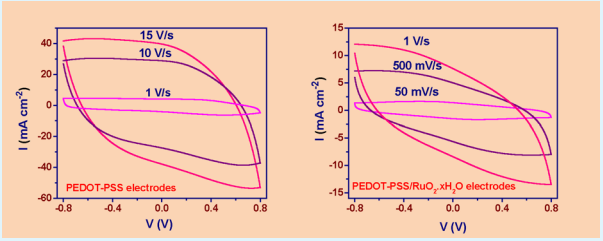

KEYWORDS: *supercapacitor, conducting polymer, hydrous ruthenium oxide, polymer electrolyte, proton conductor, impedance analysis*

1. INTRODUCTION

Supercapacitors are attractive energy storage devices exhibiting intermediate properties of high-energy-density batteries and high-power electrolytic capacitors, along with long cycle life.[1−3] These devices have excellent potential as power sources in widespread applications including electronic equipment, medical utilities, and electric vehicles like high power applications.[1−3] Charges get stored electrostatically at the interfaces of carbon electrodes and ionic conductors in the electric-double-layer capacitors (EDLCs). The carbon electrodes, employed in EDLCs, are reported to be in various forms including activated carbons,[4−6] carbon nanotubes,[4,6−8] carbon nanofibers,[4,9] graphene,[10−13] etc. The storage mechanism of translational charges is responsible for high rate performance and long cycle-life of EDLCs. Pseudocapacitors, another class of supercapacitors employ transition metal-oxides and conducting polymers as electrodes.[1,4] Fast faradaic reactions at the electrode and electrolyte interfaces are responsible to store electrical energy. Apart from the fact that pseudocapacitors offer high value of specific capacitance and various factors including insufficient reversibility and electromechanical problems during charge−discharge, pseudocapacitors offer limited performance such as low rate capability and limited cycle life.[1,4]

The candidature of conducting polymers as electrode materials for supercapacitors is inevitable because of the fast switching between oxidized and reduced states, high conductivity, environmental friendliness, low cost, and excellent mechanical properties.[1,14−17] Among diverse conducting polymers, poly(3,4-ethylenedioxythiophene) (PEDOT)-based electrodes are promising because of the unprecedented stability and faster redox transitions.[17−19] The capacitance performance in PEDOT based electrodes are mainly tested in liquid electrolytes.[18−22] However, the devices utilizing liquid electrolytes suffer from various snags for practical applicability including bulky design, leakage, corrosion in electrodes, and lack of safety. Use of quasi-solid-state gel/polymer electrolyte as an alternative is a keen approach;[5,6,23−25] however, low rate

Received: February 11, 2013
Accepted: April 2, 2013
Published: April 2, 2013

   dx.doi.org/10.1021/am4005557 | ACS Appl. Mater. Interfaces 2013, 5, 3875−3883

capability and poor frequency responses are major issues in using polymer electrolytes. High ionic resistance while diffusion of ions via polymeric network to access the active material may be attributed to poor charge−discharge rates in all-solid supercapacitors.

As mentioned above, high rate performance is generally reported in EDLCs comprising liquid or solid electrolytes. Few reports related to high rate capability in solution-based systems are available in literature.[8,12,18,26−29] Du and Pan[8] reported high rate capacitive performance in terms of high knee frequency (~7560 Hz) in electrophoretic deposited CNT electrodes. Liu and co-workers[18] have shown a high power density of 25 kW kg^{-1} of PEDOT-nanotube based supercapacitor when 80% energy density is maintained. Recently, Sheng and co-workers[12] have shown excellent rate capability of electrochemically reduced graphene oxide based EDLC with RC time constant of 1.35 ms useful for 120 Hz ac line-filtering. High rate capability in solid state supercapacitors is rarely available except a few reports. For example, Gao and Lian[30] recently presented all-solid-state capacitor based on a proton conducting polymer electrolyte and graphite electrodes exhibiting a time constant of 10 ms, which is the indicative of a high rate performance.

The present work reports the capacitive performance and rate capability studies on the flexible and quasi-solid state pseudocapacitor comprising poly (3, 4-ethylenedioxythiophene)-poly (styrene sulfonate) (PEDOT-PSS) electrodes and proton conducting polymer electrolyte. In order to improve the capacitive performance (i.e., specific capacitance, specific energy etc.) the composite electrodes of PEDOT-PSS and hydrous ruthenium oxide ($RuO_2{\cdot}xH_2O$) have been employed to fabricate the capacitor cells. It may be noted that the RuO_2 is an expensive material and its hydrate ($RuO_2{\cdot}xH_2O$) exhibits poor electronic conductivity.[31] The redox active PEDOT-PSS would provide a conducting network to $RuO_2{\cdot}xH_2O$ for binderless preparation of flexible composite electrodes. It is believed that incorporation of high redox active hydrous ruthenium oxide (with theoretical capacitance as high as 2000 F g^{-1}) to PEDOT-PSS would provide a synergic effect toward the capacitive performance when coupled with a proton conducting polymer electrolyte to form a pseudocapacitive interface.

The redox capacitors based on $RuO_2{\cdot}xH_2O$ and its composites tested in aqueous acidic electrolytes (mainly H_2SO_4 solutions) are widely reported.[32−35] The redox mechanism responsible for pseudocapacitance in hydrous RuO_2 with aqueous acidic electrolytes[32] is as follows

$$RuO_a(OH)_b + \delta H^+ + \delta e^- \leftrightarrow RuO_{a-\delta}(OH)_{b+\delta} \quad (1)$$

Lack of thermal and electrochemical stability and operating potential limited to ~1.2 V are major challenges of $RuO_2{\cdot}xH_2O$-based capacitors with aqueous acidic media. Rochefort and Pont[35] have first demonstrated pseudocapacitance in RuO_2 with nonaqueous protic ionic-liquid media, which follows the same electrochemical mechanism, mentioned above in eq 1. Though, the protic ionic-liquid addresses certain major concerns mentioned above, this is also alive to the issues like leakage, incapable in forming miniaturized and flexible devices etc. The present work employs a free-standing ionic-liquid based proton conducting polymer electrolyte as an electrolyte, which led to flexible pseudocapacitors, acceptable for practical exploitations. The flexible pseudocapacitors based on pure PEDOT-PSS and its composite with $RuO_2{\cdot}xH_2O$ have been tested with electrochemical impedance spectroscopy (EIS), cyclic voltammetry (CV), and galvanostatic charge−discharge studies.

2. EXPERIMENTAL DETAILS

2.1. Preparation and Characterization of Ionic-Liquid Polymer Electrolyte. The host polymers poly(vinyl alcohol) (PVA; average molecular weight ~124 000−186 000, 98−99% hydrolyzed) and poly(vinyl pyrrolidone) (PVP; average molecular weight ~1 300 000), and the protic ionic liquid 1-ethyl 3-methyl imidazolium hydrogen sulfate ($EMIHSO_4$) were procured from Sigma-Aldrich and used without further purification. The polymers and ionic liquid were preheated at ~80 °C overnight to avoid moisture adsorption. The ionic liquid incorporated polymer electrolyte was synthesized using "solution-cast" technique. The 0.8 g of PVP and 0.2 g of PVA were separately dissolved in 10 mL of doubly distilled water to obtain clear solutions. PVP and PVA were dissolved in water at ~25 °C and ~80 °C, respectively. These solutions were then mixed and stirred thoroughly to obtain a polymer blend of PVA and PVP. The 1:4 weight ratio of PVA:PVP was considered to be an optimized ratio of a completely miscible blend.[36] Different amount of protic ionic-liquid $EMIHSO_4$ was added to the polymer solutions and stirred thoroughly. These mixtures were then poured to flat bottom polypropylene dishes, and water was allowed to evaporate slowly at room temperature. Finally, the free-standing polymer electrolyte films were obtained and stored in argon atmosphere for the physical characterization. It was noted that the polymer electrolyte, prepared using pure PVP, was found in the form of viscous gel solution instead of free-standing film. Apart from the other benefits, the polymer PVA is acting as a stiffner to give a dimensional stability.

XRD patterns of the polymer electrolytes were recorded using X-ray diffractometer (Bruker, D8 Discover) with CuKα radiation in the Bragg angle (2θ) range from 10 to 50°. Thermal analysis of the polymer electrolytes was carried out by thermo-gravimetric analysis (TGA) and differential scanning calorimetry (DSC). TGA was performed from 30 to 600 °C at a heating rate of 10 °C min^{-1} under a dynamic dry nitrogen atmosphere using a Perkin-Elmer TGA system (TGA-7). DSC curves were recorded from room temperature to 250 °C at a heating rate of 10 °C min^{-1} in a static nitrogen atmosphere with the help of a DSC system of TA Instruments (model Q100).

The ionic conductivity of the polymer electrolyte films was evaluated from electrochemical impedance spectroscopy (EIS). The impedance spectra were recorded on the cell SS | polymer electrolyte | SS (SS: stainless steel) in a frequency range from 1 Hz to 100 kHz using an LCR meter (model 3522−50, HIOKI, Japan) at ac voltage signal of 20 mV. The electrochemical stability window (ESW) of the polymer electrolyte was estimated using cyclic voltammetry (CV) performed on the SS | polymer electrolyte | SS cell using an electrochemical analyzer (model 608C, CH Instruments, USA).

2.2. Preparation of Capacitor Electrodes. The conducting polymer PEDOT-PSS (~3 wt % content in water) and hydrous ruthenium oxide ($RuO_2{\cdot}xH_2O$) were obtained from Sigma-Aldrich and used as received. Three ml of PEDOT-PSS solution was further diluted in doubly distilled water and mechanically mixed in a mortar and pestle for few hours to form slurry. The electrodes of varying thicknesses were prepared by coating different amount of slurry on the flexible graphite sheets. For the preparation of composite electrodes, the $RuO_2{\cdot}xH_2O$ powder (~15 wt % of the total active material) was added to the water solution of PEDOT-PSS and homogeneous slurries were obtained by a thorough mechanical grinding. This slurry was also coated on the flexible graphite sheets to obtain composite electrodes. The composite electrodes are referred as PEDOT-PSS-Ru in the text. These electrodes were vacuum-dried overnight at ~80 °C before using them in capacitor cell fabrication. It may be noted that no inactive ingredient or binder was added to prepare the capacitor electrodes.

2.3. Fabrication and Characterization of Pseudocapacitors. The redox supercapacitor cells were assembled with two-electrode geometry in a specially designed cell (MTI Corporation, USA) by placing the polymer electrolyte film between symmetrical electrodes of

PEDOT-PSS or PEDOT-PSS-Ru composite electrodes. The EIS, CV, and galvanostatic charge−discharge method were used to characterize the capacitor cells. The EIS and CV measurements were recorded using electrochemical analyzer, mentioned above. The impedance spectra were taken in the frequency range from 100 kHz to 10 mHz at ac voltage signal of 20 mV.

3. RESULTS AND DISCUSSION

3.1. Properties of Polymer Electrolyte. The comparative XRD patterns of pure PVA, pure PVP, PVA-PVP blend (1:4 w/w) and PVA-PVP/$EMIHSO_4$ (1:2 w/w) polymer electrolyte films are presented in Figure 1. A peak centered at ∼20°

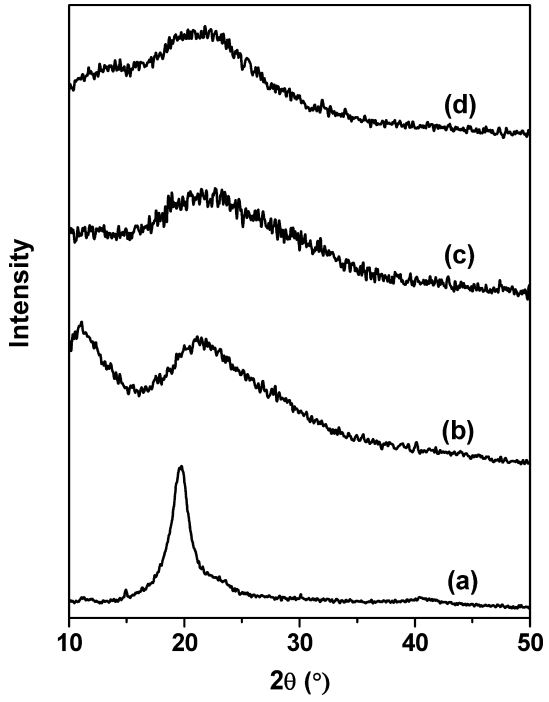

Figure 1. XRD patterns of (a) pure PVA, (b) pure PVP, (c) PVA-PVP blend (1:4 w/w) and (d) PVA-PVP/$EMIHSO_4$ (1:3 w/w).

corresponding to (110) plane for pure PVA film has been observed showing semicrystalline nature of the polymer (Figure 1a). Two broad peaks centered at ∼11 and 20° have been observed for pure PVP film indicating its amorphous nature. These two peaks disappear when it is blended with PVA and added with the ionic liquid $EMIHSO_4$ (Figure 1c, d). Instead, a broader peak centered at 21° has been observed, which shows that the crystalline phase of PVA is suppressed completely. The increase in amorphous nature is a prerequisite to obtain polymer electrolytes with higher ionic conductivity.[37]

Figure 2 shows the DSC profiles of pure PVA, pure PVP, PVA-PVP blend and PVA-PVP/$EMIHSO_4$ polymer electrolyte film. A step change due to the glass transition temperature T_g at ∼49 °C and a melting peak at T_m ∼226 °C have been observed for pure PVA (Figure 2a). The presence of melting peak confirms the semicrystalline nature of PVA. The T_g of PVP has been observed at ∼185 °C (Figure 2b). The DSC profile of PVA-PVP blend shows a single glass-transition temperature at ∼165 °C which indicates the complete miscibility of the two polymers.[38,39] On the addition of ionic-liquid $EMIHSO_4$, the T_g of PVA-PVP/$EMIHSO_4$ is found to be almost unaffected.

The TGA curves of pure PVA, pure PVP, PVA-PVP blend and PVA-PVP/$EMIHSO_4$ polymer electrolyte are shown in

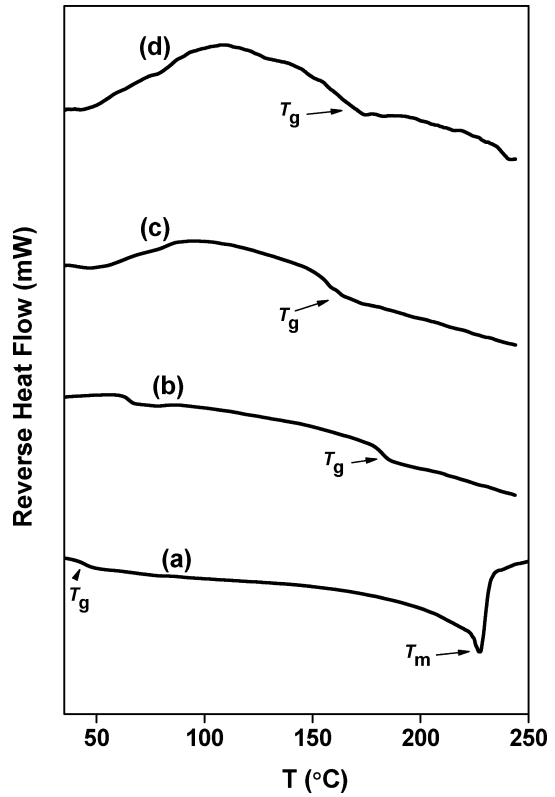

Figure 2. DSC thermogramms of (a) pure PVA, (b) pure PVP, (c) PVA-PVP blend (1:4 w/w), and (d) PVA-PVP/$EMIHSO_4$ (1:3 w/w).

Figure 3. An initial weight loss of 5 to 10 wt % has been noted for all the polymer films due to the possible loss of the

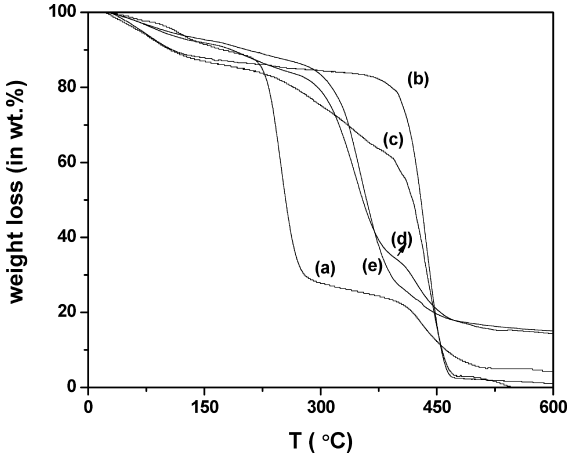

Figure 3. TGA curves of (a) pure PVA, (b) pure PVP, (c) PVA-PVP blend (1:4 w/w), (d) PVA-PVP/$EMIHSO_4$ (1:2 w/w), and (e) PVA-PVP/$EMIHSO_4$ (1:3 w/w).

adsorbed moisture. A major weight loss of PVA film has been observed at ∼230 °C due to the decomposition of low molecular weight groups of PVA.[40] On the other hand, the high thermal stability has been noted for pure PVP film with ∼80 wt % retentivity at ∼396 °C. The PVA-PVP blend shows the weight loss in two steps at ∼240 and ∼393 °C owing to the two step degradation of the polymer blend.[40] The polymer electrolytes PVA-PVP/$EMIHSO_4$ of weight ratios 1:2 and 1:3 exhibit better thermal stability. The mass retention after ∼470

°C has been observed in the case of polymer electrolyte due to the high thermal stability of ionic-liquid. The thermal stability of the polymer electrolyte up to ~280 °C is high enough for its application as electrolyte/separator in electrochemical devices.

The ionic conductivity (σ) of the PVA-PVP/$EMIHSO_4$ polymer electrolytes of different weight ratios has been estimated as shown in Figure 4. The conductivity of pure

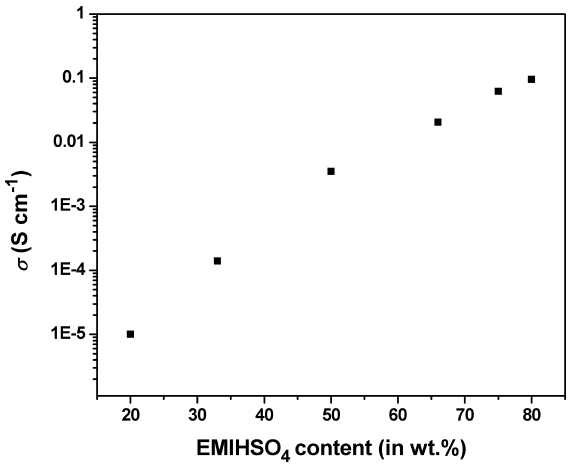

Figure 4. Conductivity variation with respect to the content of ionic-liquid $EMIHSO_4$ in PVA-PVP blends (1:4 w/w).

ionic liquid has been found to be 3.5×10^{-2} S cm^{-1} at room temperature (~20 °C). The conductivity of the polymer electrolyte increases with the increasing content of $EMIHSO_4$ and gets almost saturated with ionic-liquid content more than 70 wt %. The compositions with higher concentration of ionic-liquid (>70 wt %) are found to be fragile and difficult to handle. The PVA-PVP/$EMIHSO_4$ (1:3 w/w) is an optimized composition in terms of conductivity and mechanical stability and is used for capacitor studies. The ionic conductivity of this composition is 6.2×10^{-2} S cm^{-1} at room temperature, which is close to that of pure ionic liquid $EMIHSO_4$. The possible mobile ionic species are the component ions of ionic liquid (EMI^+ cations and HSO_4^- anions). The mobile HSO_4^- ions are the source of protonic conduction. It is established that the proton conduction in the materials mainly follows two mechanisms: (i) Grotthuss mechanism in which proton transport occurs via proton hopping between solvent molecules and protonic species, and (ii) the vehicle mechanism in which actual diffusion of protonic species takes place.[41] In the present system, the EMI^+ cations, and the multivalent anions inherently containing proton(s) like HSO_4^- ions, migrate in the viscous media of the ionic liquid.[42] However, a further investigation is needed to confirm the transport mechanism.

The CV profile of the cell SS | PVA-PVP/$EMIHSO_4$ | SS were recorded to determine the electrochemical stability window (ESW) of the polymer electrolyte (Figure 5). This parameter is important to use the polymer electrolyte in electrochemical devices including the supercapacitors. The ESW of polymer electrolyte has been found to be in the range from −1.6 to 1.7 V, which is sufficient for capacitor application.

3.2. Studies on Pseudocapacitors. Following symmetrical capacitor cells based on pure PEDOT-PSS and PEDOT-PSS-Ru composite electrodes, separated by the optimized composition of polymer electrolyte (PVA-PVP/

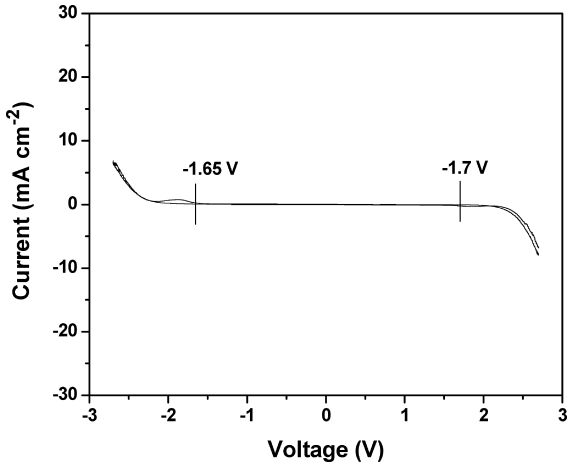

Figure 5. Cyclic voltammogram of cell SS | PVA-PVP/$EMIHSO_4$ (1:3 w/w) | SS.

$EMIHSO_4$ (1:3 w/w) have been fabricated in two-electrode configuration:

Cell#1: PEDOT-PSS | polymer electrolyte | PEDOT-PSS
Cell#2: PEDOT-PSS-Ru | polymer electrolyte | PEDOT-PSS-Ru

As mentioned earlier, the electrochemical performance of the pseudocapacitors has been examined using EIS, CV and galvanostatic charge−discharge test for numerous cycles. The EIS patterns for the capacitor cells Cell#1 and Cell#2 are depicted in panels a and b in Figure 6, respectively. It may be noted that the Z" versus Z' plots rises steeply for both the cells in the lower frequency range. These indicate the capacitive nature of the interfaces formed by pure PEDOT-PSS or PEDOT-PSS-Ru composite electrodes with the proton conducting polymer electrolyte (PVA-PVP/$EMIHSO_4$). A small semicircular portion in EIS patterns is observed for both the cells, as shown in the insets in panels a and b in Figure 6. The values of bulk resistance R_b and charge-transfer resistance R_{ct} can be evaluated from the intercepts of semicircles with Z'-axes. These parameters including overall capacitance C and specific capacitance C_{sp} have been evaluated for both the cells and listed in Table 1. The overall capacitance was evaluated using the expression: $C = (2\pi f Z'')^{-1}$, where f is the frequency of applied ac signal and Z'' is the imaginary part of the impedance Z at 10 mHz. A factor of 2 is multiplied to obtain specific capacitance C_{sp} per unit mass of the single PEDOT-PSS or its composite electrode.

The maximum theoretical specific capacitance of PEDOT is ~200 F g^{-1} depending upon the doping level of counterions, however, the experimentally observed values of specific capacitance are reported in the range of 50−80 F g^{-1}.[18,21,43] The value of C_{sp}, observed in the present case of solid -like pseudocapacitors is lower (~33 F g^{-1}). It may be noted that most of the supercapacitors reported with PEDOT-PSS electrodes are tested in liquid electrolytes (e.g., H_2SO_4 solution, etc.) which have larger accessibility of active sites of electrodes to form capacitive interfaces. The limited accessibility of quasi-solid-state gel electrolyte to form capacitive interfaces with the active sites of the electrode material results in reduced capacitance values. In an earlier report, a relatively lower specific capacitance value (~2 mF cm^{-2}) has been obtained in high rate solid-state supercapacitor using graphite electrodes and proton conducting polymer electrolyte PVA-SiWA-

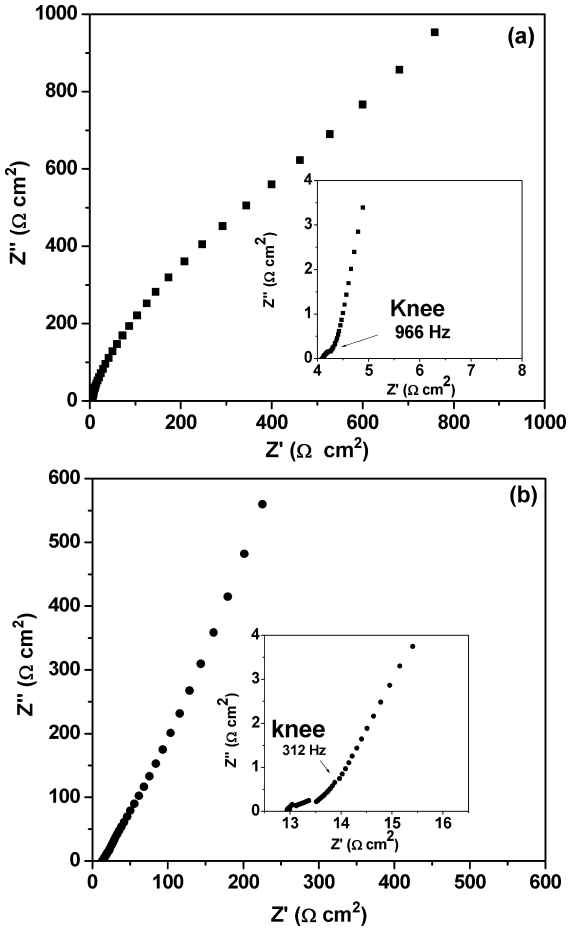

Figure 6. Impedance plots of (a) Cell#1 and (b) Cell#2.

Table 1. Various Electrical Parameters of the Capacitor Cells from Impedance Analysis

capacitor cells	R_b (Ω cm^2)	R_{ct} (Ω cm^2)	R at 10 mHz (Ω cm^2)	C (mF cm^{-2})	C_{sp} (F g^{-1})
Cell#1	4.0	0.3	760	17	33
Cell#2	12.8	0.3	223	28	57

H_3PO_4.[30] The other beneficial aspects of the solid-like configuration of capacitor cells to form leakage free, moldable and safe devices are crucial for practical exploitations.

About 72% enhancement in the value of C_{sp} has been observed for the Cell#2 with respect to Cell#1 due to the incorporation of hydrous RuO_2 in the PEDOT-PSS electrode. This leads to the enhancement in specific energy of the capacitor cell with the same proportion. This noteworthy improvement in the specific capacitance due to the composite electrodes shows the compatibility of hydrous-RuO_2 active material with the nonaqueous proton conducting polymer electrolyte. Huang et al.[44] reported the PEDOT-PSS-$RuO_2{\cdot}xH_2O$ composite electrodes showing high specific capacitance of 653 F g^{-1} with aqueous H_2SO_4 as electrolyte; however, the rate performance of such system appears to be low as the CV was recorded at low scan rate only. There are few limitations about the usage of aqueous electrolytes in supercapacitors.[35] These include the unsafe operation at elevated temperatures and the working potential range (limited to ∼1.2 V). Replacement with nonaqueous protic ionic liquid dealt with the above-mentioned issues as reported by Rochefort and Pont;[35] however, such a device offered a relatively low value of specific capacitance of 83 F g^{-1} for thermally prepared RuO_2. The low value of capacitance has been explained on the basis of limited accessibility of active electrode sites in viscous ionic-liquid media.[35] In an another report, a solid-state asymmetric supercapacitor comprising graphite and RuO_2 electrodes, and nonaqueous proton conducting polymer electrolyte (PVA–heteropoly acid) exhibits a total specific capacitance (including double layer and pseudocapacitance) of 24 mF cm^{-2}.[45]

The rate capability is another important aspect of consideration to design a high power supercapacitor.[46] The high rate performance can be estimated from the impedance analysis in terms of the knee frequency and/or the response time, the Miller's approach.[46,47] The knee frequency of a capacitor is the on-set frequency below which the capacitive behavior of the cell is dominant and hence the imaginary impedance Z'' rises steeply with respect to the real part (Z') of the impedance.[26] The estimated values of knee frequency for both the cells are listed in Table 2. An exceptionally high knee

Table 2. Rate Performance Characteristics of the Capacitor Cells from Impedance Analysis

capacitor cells	knee freq, f_{knee} (Hz)	response freq, f_0 (Hz)	response time, τ_0 (s)	available energy, E_0 (W h kg^{-1})	pulse power, figure-of-merit (kW kg^{-1})
Cell#1	966	14	0.07	0.2	10.2
Cell#2	312	1	1	0.9	3.2

frequency of ∼966 Hz has been observed for Cell#1, which indicates a fast switching behavior at the interfaces of PEDOT-PSS electrodes and the proton conducting electrolyte PVA-PVP/$EMIHSO_4$. Such a high value of knee frequency indicates the high power delivering ability of Cell#1 comprising PEDOT electrodes in combination with nonaqueous proton conducting electrolyte.

About one-third reduction in the knee frequency value has been observed (Table 2) when the composite electrodes PEDOT-PSS-Ru are employed to fabricate the capacitor Cell#2. This suggests that the presence of hydrous RuO_2 slows down the protonation–deprotonation kinetics at the interfaces of composite electrodes and proton conducting electrolyte. Hence, a relatively reduced power level of the capacitor cell (Cell#2) has been observed. It may be noted that even after substantial reduction, the knee frequency of the present composite electrode system is remarkably high (312 Hz). This is attributed to excellent electronic network provided by the conducting polymer PEDOT-PSS responsible for facile protonic and electronic conduction through $RuO_2{\cdot}xH_2O$ particles. Many workers reported such electronic networks by adding carbonaceous materials, e.g., vapor grown carbon fiber (VGCF),[48] carbon nanofiber (CNF),[49] etc. However, the rate capabilities of such systems are not as high as reported in the present system.

As mentioned above, the response time (τ_0) is another parameter which indicates the rate performance of a capacitor.[46] It is the reciprocal of the response frequency f_0 at which the real and imaginary part of impedance Z as a function of frequency cross each other or in other words the resistive and capacitive contributions to the total impedance are equal. At this frequency f_0, the phase difference between real and imaginary part of Z is 45°.[47] The Z' and Z'' plots as a

dx.doi.org/10.1021/am4005557 | ACS Appl. Mater. Interfaces 2013, 5, 3875–3883

function of frequency are shown in panels a and b in Figure 7 for Cell#1 and Cell#2, respectively. Their response times are

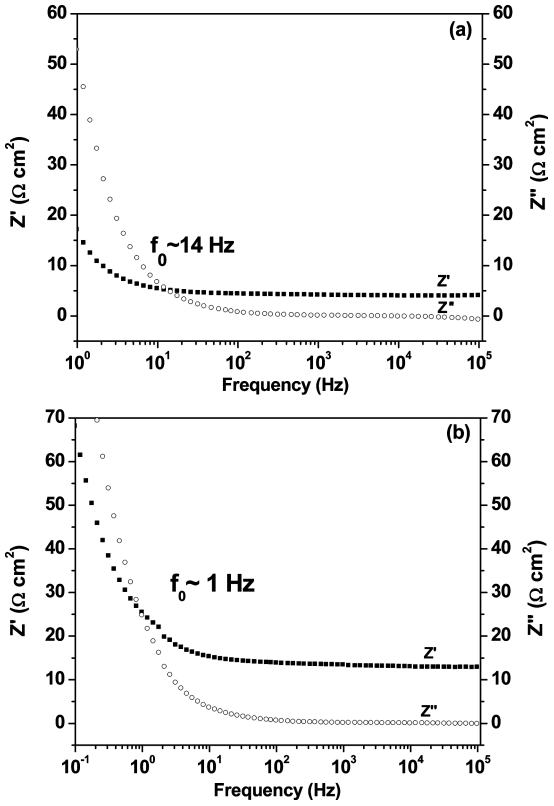

Figure 7. Bode plots of the capacitor cells: (a) Cell#1 and (b) Cell#2.

listed in Table 2. The response times are directly associated with the pulse power performance (also referred as figure-of-merit) of the capacitors which can be estimated from the available energy density E_0 at f_0 divided by the response time.[47] The values of pulse power estimated for both the cells are also listed in Table 2. The comparative values of response times indicate that Cell#2 delivers a slower response with respect to that of Cell#1. This is possible due to slow protonation–deprotonation process associated with the composite electrodes (containing $RuO_2 \cdot xH_2O$) relative to the charge transfer process of pure PEDOT/electrolyte interfaces. Thus, the deterioration in the pulse power performance has been observed due to the employment of PEDOT-$RuO_2 \cdot xH_2O$ composite electrodes.

The performance characteristics of the two capacitor cells (Cell#1 and Cell#2) have also been evaluated by cyclic voltammetry. Panels a and b in Figure 8 depict the comparative CV responses of the cells, Cell#1 and Cell#2, respectively, at a scan rate of 200 mV s^{-1} recorded at room temperature. Substantially higher voltammetric current and hence the higher specific capacitance has been observed for the Cell#2 (with composite electrodes) as compared to that for the Cell#1 (with PEDOT electrodes). This is the direct indicative of the capacitive role of $RuO_2 \cdot xH_2O$ incorporated in the PEDOT-PSS electrodes. In order to evaluate the rate capability of the capacitor cells Cell#1 and Cell#2, the CV responses have been recorded for varying scan rates, as shown in Figure 9a and b, respectively. It may be noted that the rectangular shape of the voltammograms for the Cell#1 are maintained up to the high scan rate 15 V s^{-1}. This further indicates a substantially high rate performance of the PEDOT-PSS electrodes coupled with

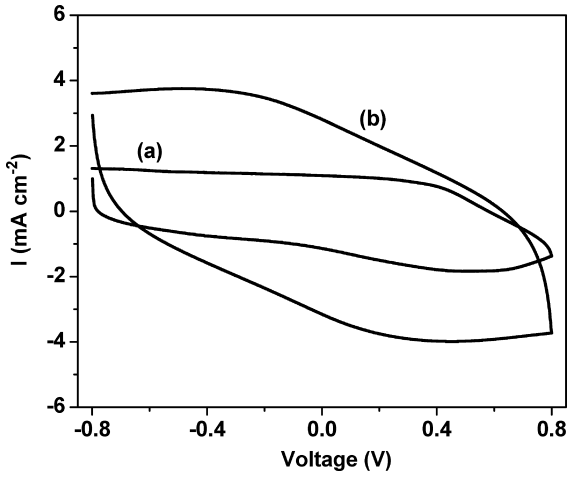

Figure 8. Cyclic voltammograms of the capacitor cells (a) Cell#1 and (b) Cell#2 at the scan rate of 200 mV s^{-1}.

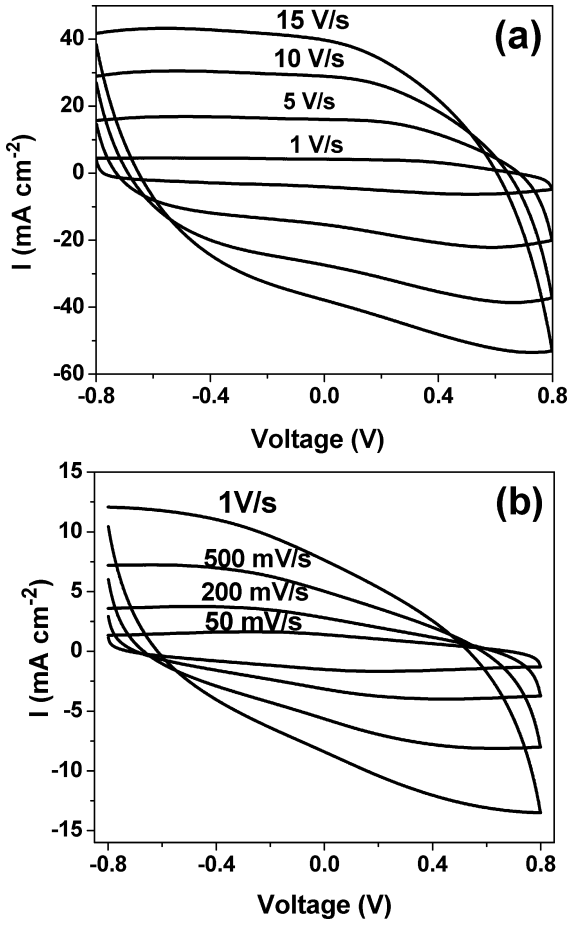

Figure 9. Cyclic voltammograms of the capacitor cells (a) Cell#1, and (b) Cell#2 at different scan rates.

the proton conducting electrolyte. The high rate performance of the cell was indicated from impedance studies, discussed earlier. A very few reports on high rate performance of the capacitors are available in literature. For example, Gao and Lian[30] reported rectangular CV response up to 20 V s^{-1} for an EDLC with graphite electrodes and PVA-based proton conducting electrolyte. In another study, Liu et al.[18] reported the high rate performance (CV reported up to 1000 mV s^{-1}) of

dx.doi.org/10.1021/am4005557 | ACS Appl. Mater. Interfaces 2013, 5, 3875–3883

a redox capacitor comprising PEDOT-nanotubes as electrodes with liquid electrolyte (1 M $LiClO_4$). To the best of our knowledge, the present study is a first report on a quasi-solid-state redox (pseudo-) capacitor with such a high rate performance.

Figure 9b shows the CV responses of the Cell#2 based on PEDOT-PSS-Ru composite electrodes at different scan rates. With the incorporation of $RuO_2{\cdot}xH_2O$ in composite electrode, a deviation from quasi-rectangular shape of CV has been observed beyond the scan rate of 500 mV s^{-1}. This further shows the reduced rate capability of composite electrodes which is in accordance with the results obtained in impedance plots. The capacitive CV responses of bulk $RuO_2{\cdot}xH_2O$ are generally reported for the lower scan rates, showing low rate capability.[50] In order to improve the rate performance, few composite electrodes of $RuO_2{\cdot}xH_2O$ are reported, which show rectangular CV responses up to the scan rate of 400−500 mV s^{-1}.[51,52] This is due to the improved pathways for electronic and protonic conduction due to the incorporation of suitable conducting networks.[51] In the present case also, the conducting polymer PEDOT-PSS acts as an excellent conducting network to provide pathways for electron and proton exchanges through $RuO_2{\cdot}xH_2O$, which improves the rate capability of the composite electrodes.

The comparative performance of PEDOT-PSS and its composite with hydrous RuO_2 as capacitor electrodes has been studied by constant current charge−discharge tests also. The charge−discharge profiles of Cell#1 with PEDOT-PSS and Cell#2 with PEDOT-PSS-Ru electrodes at a constant current of 0.1 mA cm^{-2} are presented in profiles a and b in Figure 10,

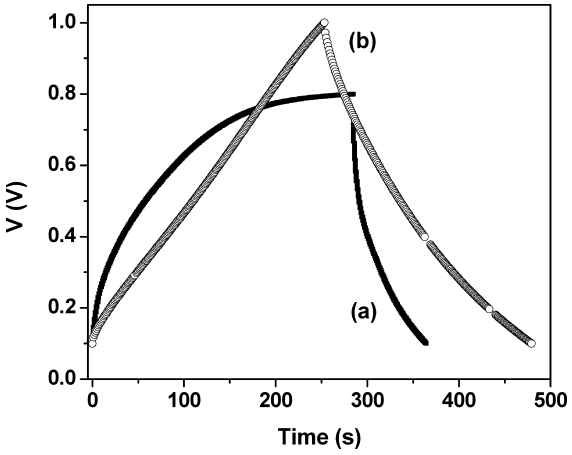

Figure 10. Charge−discharge profiles of the capacitor cells (a) Cell#1 and (b) Cell#2 at the current 0.1 mA cm^{-2}.

respectively. It has been observed that the cell with pure PEDOT-PSS electrodes has been charged up to the potential of 0.8 V, whereas the charging potential has been slightly increased to 1.0 V with the composite electrodes. This suggests that the dominant protonation−deprotonation processes at the composite electrodes/proton conducting electrolyte interfaces are due to the presence of $RuO_2{\cdot}xH_2O$.

The discharge capacitance C_d of the two cells has been evaluated using the equation $C_d = (i\Delta t)/(m\Delta V)$, where i is the applied constant current, m is the mass of the active electrode material, and $\Delta V/\Delta t$ is the slope of the linear part of discharge curves (Figure 10) and the values are listed in Table 3. The capacitance value due to PEDOT-PSS electrodes and its

Table 3. Charge−Discharge Characteristics of the Capacitor Cells at the Current 0.1 mA cm^{-2}

capacitor cells	*ESR* (Ω cm^2)	discharge capacitance, C_d (mF cm^{-2})	discharge capacitance, C_d (F g^{-1})	specific energy *E* (W h kg^{-1})	specific power *P* (W kg^{-1})
Cell#1	626	14.8	30	0.6	216
Cell#2	279	31	62	2.0	846

enhancement due to the composite electrodes are consistent with the values estimated from the EIS and CV techniques. The other important parameter namely the equivalent series resistance (ESR) has been estimated from the sudden initial drop of the discharge profile and given in Table 3. The specific energy E and power density P of the capacitor cells have also been evaluated using the following relations and listed in Table 3

$$E = \frac{C_d V^2}{2m} \tag{2}$$

$$P = \frac{V^2}{4mESR} \tag{3}$$

where V is the voltage range of charge−discharge excluding the IR drop and m is the mass of the active material in the single electrode.

The discharge characteristics of the capacitor cells Cell#1 and Cell#2 with different current densities are shown in panels a and b in Figure 11, respectively. About 50% fading in the specific capacitance of Cell#1 (with PEDOT-PSS electrodes) has been observed when load current varies from 0.1 to 0.4 mA cm^{-2}. On the other hand, only 11% fading in specific capacitance has been noted for Cell#2 comprising PEDOT-PSS-Ru composite electrodes with the same increase in current. This indicates the effective capacitive role of $RuO_2{\cdot}xH_2O$ in the composite electrodes.

The ESR value of the capacitor cell (Cell#2) has been reduced by almost half when PEDOT-PSS-Ru composite electrodes have been employed (Table 3). The values of *ESR* have been found to be comparable with the overall values of resistance recorded at 10 mHz in the impedance plots. (Table 1) The slightly higher value of charging voltage and substantial reduction in ESR value of composite electrodes-based capacitor cell (Cell#2) are responsible for noteworthy improvement in power density of the capacitor (Table 3). The power density of Cell#1 with pure PEDOT-PSS electrode has been found to be ∼216 W kg^{-1}, which is a low value from a supercapacitor point-of-view. Actually, the PEDOT-PSS does not swell in organic media and exhibits high ionic resistance, resulting in the low specific power values.[43] Various reports on modifications of PEDOT-PSS electrodes to improve its power density are present in literature.[43] The ionic motion has been enhanced when PEDOT-PSS is blended with PEO exhibiting a power density of 100 W kg^{-1}.[43] In another report, much higher power density values (up to 3 kW kg^{-1}) are shown in PEDOT-PSS/PPy composites.[43] In the present system, about 3-fold improvement in power density has been obtained when $RuO_2{\cdot}xH_2O$ is added to PEDOT-PSS material. Fast kinetics of the electrochemical processes involved is attributed to higher specific power values achieved in the present system.

dx.doi.org/10.1021/am4005557 | ACS Appl. Mater. Interfaces 2013, 5, 3875−3883

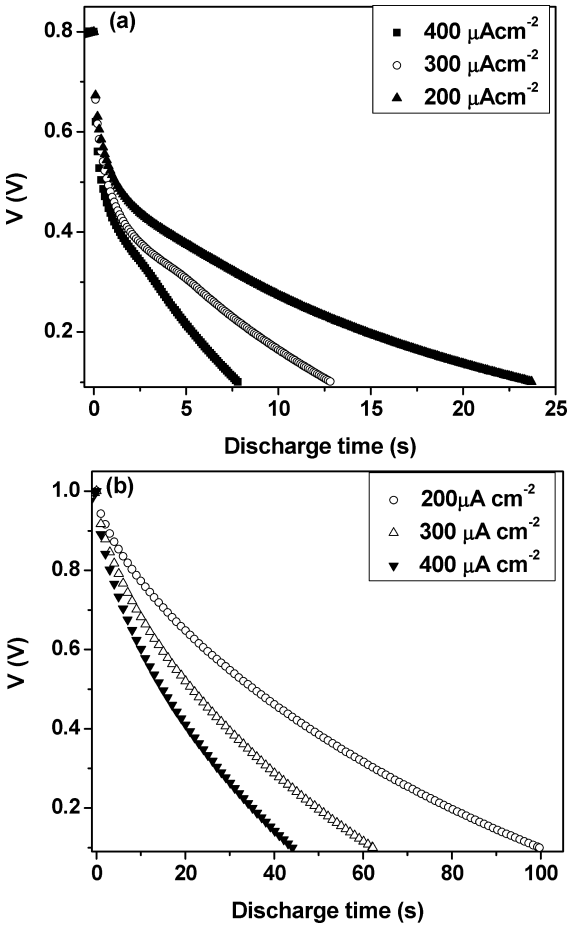

Figure 11. Discharge profiles of the capacitor cells (a) Cell#1 and (b) Cell#2 at different load currents.

Figure 12 shows the capacitance variation as a function of charge–discharge cycles for Cell#2 (with composite electrodes)

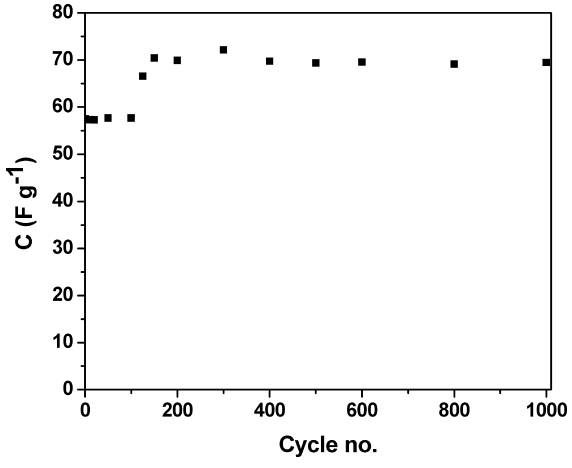

Figure 12. Variation of specific capacitance with respect to number of charge–discharge cycles for Cell#2.

recorded for 1000 cycles. About 15% improvement in the specific capacitance has been observed for the first few cycles (~200 cycles) and thereafter, almost stable capacitance (~70 F g^{-1}) has been achieved. In general, the EDLCs/pseudocapacitors show a fading in capacitance, because of the consumption of charges due to irreversible electrochemical reaction(s) with adsorbed surface groups like OH^- species etc.[5,21,23,53] But, the improvement in capacitance for initial charge–discharge cycles are rarely reported. Our group reported such behavior in redox supercapacitor fabricated with 1,5-diaminoanthraquinone (DAAQ) electrodes and PVA-H_3PO_4 polymer electrolyte film.[54] Cheng et al.[55] observed similar result in graphene-based supercapacitor and termed this phenomenon as electro-activation where ions tend to adjust with cycling to fully access the active electrode material.

4. CONCLUSIONS

Studies are presented on the novel solid-state and flexible pseudocapacitors using protic ionic liquid based polymer electrolyte with PEDOT-PSS and composite PEDOT-PSS/$RuO_2{\cdot}xH_2O$ electrodes. High ionic conductivity (~6.2×10^{-2} S cm^{-1} at 20 °C), sufficient thermal stability and the structural properties of PVA-PVP/$EMIHSO_4$ electrolyte show its suitability in capacitor devices. Pseudocapacitors with Symmetrical configuration using PEDOT-PSS and composite PEDOT-PSS/$RuO_2{\cdot}xH_2O$ electrodes have been fabricated and characterized using EIS, CV and charge–discharge tests. The PEDOT-PSS/$RuO_2{\cdot}xH_2O$ composite electrodes show enhanced specific capacitance (~57 F g^{-1}) over pure PEDOT-PSS electrodes (~33 F g^{-1}), indicating the effective role of protonation–deprotonation of $RuO_2{\cdot}xH_2O$ entrapped in conducting network of PEDOT-PSS. This enhancement in capacitance also indicates the compatibility of hydrous RuO_2 with the proton conducting polymer electrolyte. Various observations like high knee frequency in impedance plot, low response time (hence high pulse power) and capacitive CV response for high scan rates indicate the high rate capability of capacitive interfaces formed with PEDOT-PSS electrodes and proton conducting electrolyte. The incorporation of $RuO_2{\cdot}xH_2O$ in PEDOT-PSS network deteriorates its high rate performance; however, the composite electrode shows its rate capability higher than many capacitive interfaces of the $RuO_2{\cdot}xH_2O$ composites with carbonaceous or oxide materials. The specific energy and power have also been improved substantially when PEDOT-PSS/$RuO_2{\cdot}xH_2O$ composite electrodes are employed for pseudocapacitor cells, as observed from charge–discharge studies. Stable capacitance of ~70 F g^{-1} with PEDOT-PSS composite electrodes has been observed for 1000 charge–discharge cycles, after initial improvement in the specific capacitance.

AUTHOR INFORMATION

Corresponding Author

*E-mail: sahashmi@physics.du.ac.in. Tel.: +911127604881. Fax: +911127667061.

Notes

The authors declare no competing financial interest.

ACKNOWLEDGMENTS

The authors acknowledge the financial support received from the Department of Science & Technology, New Delhi (Sanction DST/TSG/PT/2009/93) and University of Delhi (11-17 Research Fund).

REFERENCES

(1) Conway, B. E. In *Electrochemical Supercapacitors, Scientific Fundamentals and Technological Applications*; Kluwer Academic/Plenum: New York, 1999.

(2) Winter, M.; Brodd, R. J. *Chem. Rev.* **2004**, *104*, 4245−4269.
(3) Simon, P.; Gagotsi, Y. *Nat. Mater.* **2008**, *7*, 845−854.
(4) Wang, G.; Zhang, L.; Zhang, J. *Chem. Soc. Rev.* **2012**, *41*, 797−828.
(5) Pandey, G. P.; Hashmi, S. A.; Kumar, Y. *Energy Fuels* **2010**, *24*, 6644−6652.
(6) Kumar, Y.; Pandey, G. P.; Hashmi, S. A. *J. Phys. Chem. C* **2012**, *116* (50), 26118−26127.
(7) Pan, H.; Li, J.; Feng, Y. P. *Nanoscale Res. Lett.* **2010**, *5*, 654−668.
(8) Du, C.; Pan, N. *J. Power Sources* **2006**, *160*, 1487−1494.
(9) Barranco, V.; Lillo-Rodenas, M. A.; Linares-Solano, A.; Oya, A.; Pico, F.; Ibanez, J.; Agullo-Ruedo, F.; Amarilla, J. M.; Rojo, J. M. *J. Phys. Chem. C* **2010**, *114*, 10302−10307.
(10) Stoller, M. D.; Park, S.; Zhu, Y.; An, J.; Ruoff, R. S. *Nano Lett.* **2008**, *8* (10), 3498−3502.
(11) Biswas, S.; Drzal, L. T. *ACS Appl. Mater. Interfaces* **2010**, *2* (8), 2293−2300.
(12) Sheng, K.; Sun, Y.; Li, C.; Yuan, W.; Shi, G. *Sci. Rep.* **2012**, DOI: 10.1038/srep 00247.
(13) Wang, Y.; Shi, Z.; Huang, Y.; Ma, Y.; Wang, C.; Chen, M.; Chen, Y. *J. Phys. Chem. C* **2009**, *113*, 13103−13107.
(14) Wang, K.; Huang, J.; Wei, Z. *J. Phys. Chem. C* **2010**, *114*, 8062−8067.
(15) Aradilla, D.; Estrany, F.; Aleman, C. *J. Phys. Chem. C* **2011**, *115*, 8430−8438.
(16) Inzelt, G. In *Conducting Polymers: A New Era in Electrochemistry*; Springer Verlag: Berlin, 2008.
(17) Snook, G. A.; Kao, P.; Best, A. S. *J. Power Sources* **2011**, *196*, 1−12.
(18) Liu, R.; Cho, S.; Lee, S. B. *Nanotechnology* **2008**, *19*, 215710 (8pp).
(19) Chu, C-Y; Tsai, J-T; Sun, C-L; Int, J. *Hydrogen Energy* **2012**, DOI: 10.1016/j.ijhydene.2012.05.017.
(20) Huang, Li-M; Wen, T-C; Gopalan, A. *Electrochim. Acta* **2006**, *51*, 3469−3476.
(21) Chen, Li; Yuan, C.; Dou, H.; Gao, B.; Chen, S.; Zhang, X. *Electrochim. Acta* **2009**, *54*, 2335−2341.
(22) Alvi, F.; Ram, M. K.; Basnayaka, P. A.; Stefanakos, E.; Goswami, Y.; Kumar, A. *Electochim. Acta* **2011**, *56*, 9406−9412.
(23) Hashmi, S. A. *Natl. Acad. Sci. Lett.* **2004**, *27*, 27−46.
(24) Yuan, L.; Lu, X.-H.; Xiao, X.; Zhai, T.; Dai, J.; Zhang, F.; Hu, B.; Wang, X.; Gong, L.; Chen, J.; Hu, C.; Tong, Y.; Zhou, J.; Wang, Z. L. *ACS Nano* **2012**, *6* (1), 656−661.
(25) Lufrano, F.; Staiti, P. *Energy Fuels* **2010**, *24*, 3313−3320.
(26) Du, C.; Pan, N. *Nanotechnology* **2006**, *17*, 5314−5318.
(27) Miller, J. R.; Outlaw, R. A.; Holloway, B. C. *Science* **2010**, *329*, 1637−1639.
(28) Pech, D.; Brunet, M.; Durou, H.; Huang, P.; Mochalin, V.; Gogotsi, Y.; Taberna, P. L.; Simon, P. *Nat. Nanotechnol. Lett.* **2010**, 651−654.
(29) Korenblit, Y.; Rose, M.; Kockrick, E.; Borchardt, L.; Kvit, A.; Kaskel, S.; Yushin, G. *ACS Nano* **2010**, *4* (3), 1337−1344.
(30) Gao, H.; Lian, K. *J. Power Sources* **2011**, *196*, 8855−8857.
(31) Sugimoto, W.; Iwata, H.; Yokoshima, K.; Murakami, Y.; Takasu, Y. *J. Phys. Chem. B* **2005**, *109*, 7330−7338.
(32) Hu, C. C.; Liu, M. J.; Chang, K. H. *Electrochim. Acta* **2008**, *53*, 2679−2687.
(33) Song, R. Y.; Park, J. H.; Sivakkumar, S. R.; Kim, S. H.; Ko, J. M.; Park, D. Y.; Jo, S. M.; Kim, D. Y. *J. Power Sources* **2007**, *166*, 297−301.
(34) Liu, R.; Duay, J.; Lane, T.; Lee, S. B. *Phys. Chem. Chem. Phys.* **2010**, *12*, 4309−4316.
(35) Rochefort, D.; Pont, A. L. *Electrochem. Commun.* **2006**, *8*, 1539−1543.
(36) Zhang, X.; Takegoshi, K.; Hikichi, K. *Polymer* **1992**, *33* (4), 712−717.
(37) Gray, F. M. In *Solid Polymer Electrolyte: Fundamentals and Technology Applications*; VCH Publishers: New York, 1991; p 83.
(38) Seabra, A. B.; de Oliveira, M. G. *Biomaterials* **2004**, *25*, 3773−3782.
(39) Cassu, S. N.; Felisberti, M. I. *Polymer* **1997**, *38* (15), 3907−3911.
(40) Subramania, A.; Kalyana Sundaram, N. T.; Sukumar, N. *J. Power Sources* **2005**, *141*, 188−192.
(41) Raducha, D.; Wieczorek, W.; Florjańczyk, Z.; Stevens, J. R. *J. Phys. Chem.* **1996**, *100*, 20126−20133.
(42) Ogihara, W.; Kosukegawa, H.; Ohno, H. *Chem. Commun.* **2006**, DOI: 10.1039/b606186a.
(43) Snook, G. A.; Kao, P.; Best, A. S. *J. Power Sources* **2011**, *196*, 1−12.
(44) Huang, L.-M.; Lin, H.-Z.; Wen, T.-C.; Gopalan, A. *Electrochim. Acta* **2006**, *52*, 1058−1063.
(45) Lian, K.; Tian, Q. *Electrochem. Commun.* **2010**, *12*, 517−519.
(46) Miller, J. R. In *Proceedings of the Eighth International Seminar on Double Layer Capacitors and Similar Energy Storage Devices*; Deerfield Beach, FL, Dec 7−9, 1998 ; Florida Educational Seminars: Boca Raton, FL, 1998.
(47) Lufrano, F.; Staiti, P.; Minutoli, M. *J. Power Sources* **2003**, *124*, 314−320.
(48) Lee, B. J.; Sivakkumar, S. R.; Ko, J. M.; Kim, J. H.; Jo, S. M.; Kim, D. Y *J. Power Sources* **2007**, *168*, 546−552.
(49) Chuang, C.-M.; Huang, C.-W.; Teng, H.; Ting, J.-M. *Compos. Sci. Technol.* **2012**, *72*, 1524−1529.
(50) Lin, K.-M.; Chang, K.-H.; Hu, C.-C.; Li, Y.-Y. *Electrochim. Acta* **2009**, *54*, 4574−4581.
(51) Hu, C.-C.; Wang, C.-W.; Wu, T.-H.; Chang, K.-H. *Electrochim. Acta* **2012**, *85*, 90−98.
(52) Hseieh, T.-F.; Chuang, C.-C.; Chen, W.-J.; Huang, J.-H.; Chen, W.-T.; Shu, C.-M. *Carbon* **2012**, *50*, 1740−1747.
(53) Hashmi, S. A.; Latham, R. J.; Linford, R. G.; Schlindwein, W. S. *Polym. Int.* **1998**, *47*, 28−33.
(54) Hashmi, S. A.; Suematsu, S.; Naoi, K. *J. Power Sources* **2004**, *137*, 145−151.
(55) Cheng, Q.; Tang, J.; Ma, J.; Zhang, H.; Shinya, N.; Qin, L-C *Carbon* **2011**, *49*, 2917−2925.